

ELECTRONIC SUPPORTING INFORMATION

Cooperative spin crossover phenomena in $[\text{Fe}(\text{NH}_2\text{trz})_3](\text{tosylate})_2$ nanoparticles

Alexey Tokarev,^a Lionel Salmon,^a Yannick Guari,^b William Nicolazzi,^a Gábor Molnár,^a and Azzedine Bousseksou^{*a}

^a*Laboratoire de Chimie de Coordination, CNRS UPR-8241 and Université de Toulouse ; UPS, INP ; F-31077 Toulouse, France.*

Fax: +33(0)561553003, e-mail: azzedine.bousseksou@lcc-toulouse.fr

^b*Institut Charles Gerhardt Montpellier, UMR5253, Chimie Moléculaire et Organisation du Solide, Université Montpellier II, Place E. Bataillon, 34095, Montpellier cedex 5, France.*

S2: 1. Materials

S2: 2. Preparation of Nanoparticles

S2-S3: 3. Characterization

S4-S5: 3.1. TEM measurements

S6-S8: 3.2. DLS measurements

S9: 3.3. UV absorption spectra

S10-S12: 3.4. Magnetic properties

S13: 3.5. Mössbauer spectra

S14: 4. References

1. Materials

Iron powder for preparing hexaquoiron(II)-p-toluenesulfonate was purchased from Alfa Aesar. Hexaquoiron(II)-p-toluenesulfonate was synthesised as described previously [1]. Secondary alcohol ethoxylate 15-S-3 from Dow Chemical Co. (>97% purity) was chosen as nonionic surfactant to form a reverse micelle system. All solvents were obtained from commercial sources as analytical grade and used without further purification.

2. Preparation of Nanoparticles

Firstly two microemulsions were prepared by adding the iron precursor (0.125g, 0.25 mmol) in a methanol-water (0.4 ml) solution with ascorbic acid and a 4-amino-1,2,4-triazole (0.063g, 0.75 mmol) aqueous solution (0.2 ml) to two equal volumes of the surfactant (5+5 ml) and stirred. The obtained microemulsions were vigorously mixed together for 10 min and subjected to either slow vacuum evaporation at ambient temperature **1** or solid extraction **2**. Separation of the nanoparticles **2** from the final microemulsion involves: immediate destabilisation of the microemulsion by diethyl ether (*ca.* 160 ml), further extraction of the particles by centrifugation, extensive washing with the same solvent and vacuum drying. Nanoparticles **2** were obtained as a pink powder with yield of 70 %. Sample **3** was prepared by slowly heating solution **1** to 353 K and maintaining at this temperature for 5 h.

3. Characterization

Particle size and size distribution were determined by transmission electron microscopy (TEM) using either a JEOL JEM-1010 (accelerating voltage of 100 kV) or a JEOL JEM-2100F instrument (HRTEM, accelerating voltage of 200 kV). TEM samples were prepared by placing on a carbon coated copper grid either a drop of the nanoparticles **2** suspended in a solvent or ultrathin-section of the dispersed colloids **1**, **3** using cryo-microtomy. The temperature dependent dynamic light scattering (DLS) measurements were observed on a Zetasizer Nano-S (Malvern Instrument, UK). A He-Ne laser at $\lambda=632$ nm was used as a light source and the scattering angle was 173°. The results of scattering data were analyzed *via* a non-negative least squares algorithm (GP) as implemented in the Zetasizer Nano software [2]. Viscosity was measured on a stress-controlled rheometer (TA Instruments AR 1000) with a cone (40 and 60 mm diameter, 2° cone angle) from 293 to 313 K. Refractive index was

measured on an Abbe refractometer (OPL, France) at different temperatures. Ultraviolet-visible absorbance spectra were recorded on a Cary 50 spectrophotometer equipped with a thermostated cell holder. Magnetic susceptibility measurements were performed on a Quantum Design model MPMS2 magnetometer operating at 1 K min^{-1} under 10000 Oe magnetic field. After each warming the sample was held at the highest temperature for 40 min. ^{57}Fe Mössbauer spectra were recorded using a conventional constant-acceleration type spectrometer equipped with a 50 mCi ^{57}Co source and a flow-type, liquid helium cryostat. Before measurements sample **2** was heated to 378 K and spectra were recorded at 317 and 80 K. Least-squares fitting of the Mössbauer spectra was carried out with the assumption of Lorentzian line shapes by using the Recoil software package. The mass spectra were recorded using ElectroSpray Ionisation in both positive and negative mode on a Q-Tof I (Micromass, Manchester, UK) apparatus. IR spectra were recorded on a Perkin Elmer 1725 spectrometer with a 4 cm^{-1} resolution. Elemental analysis was carried out on a Flash EA 1112 (ThermoFinnigan 2003) apparatus.

Nanoparticles **2**. Mass spectrum: $[\text{M} - \text{C}_{13}\text{H}_{19}\text{FeN}_{12}\text{O}_3\text{S}]^-$ at $\text{m/z} = 171.0$; $[\text{M} - \text{C}_{14}\text{H}_{14}\text{O}_6\text{S}_2]^+$ at $\text{m/z} = 309.1$; $[\text{M} - \text{C}_{14}\text{H}_{14}\text{FeO}_6\text{S}_2]^+$ at $\text{m/z} = 251.0$. IR (ATR, cm^{-1}): 681, 709, 814, 1008, 1032, 1100, 1124, 1173, 1496, 1545, 1638, 3103, 3214, 3286. Elemental analysis: Found: C, 35.42; H, 4.70; N, 22.69; S, 9.16. Calcd: C, 34.99; H, 4.40; N, 24.48; S, 9.34.

3.1. TEM measurements

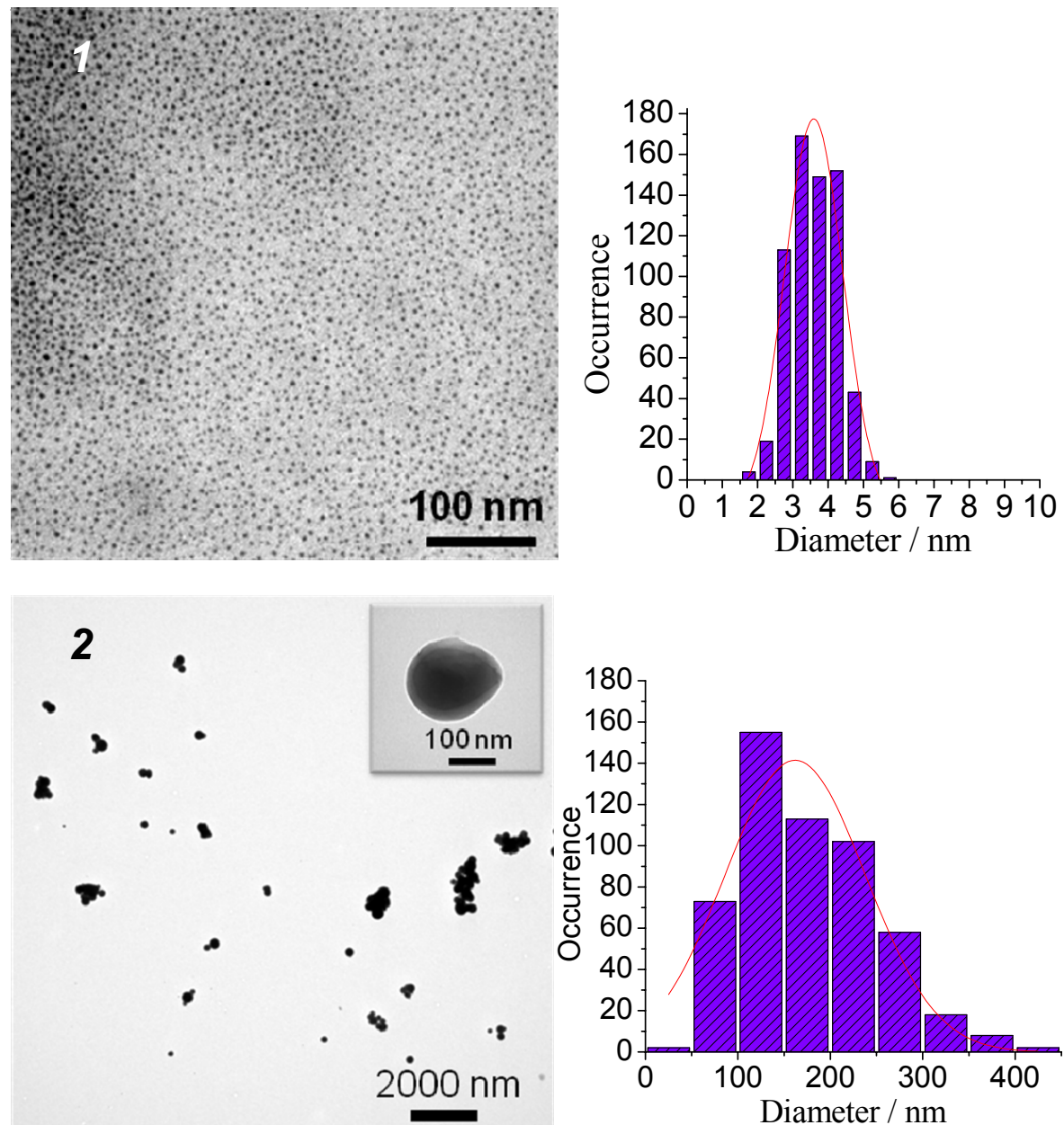


Fig. S1 Cryo-microtomy TEM (upper panel) of the $[\text{Fe}(\text{NH}_2\text{trz})_3](\text{tos})_2$ nanoparticles in a surfactant matrix **1** and TEM (lower panel) images of the particles obtained after precipitation **2**. The corresponding size distributions are also shown.

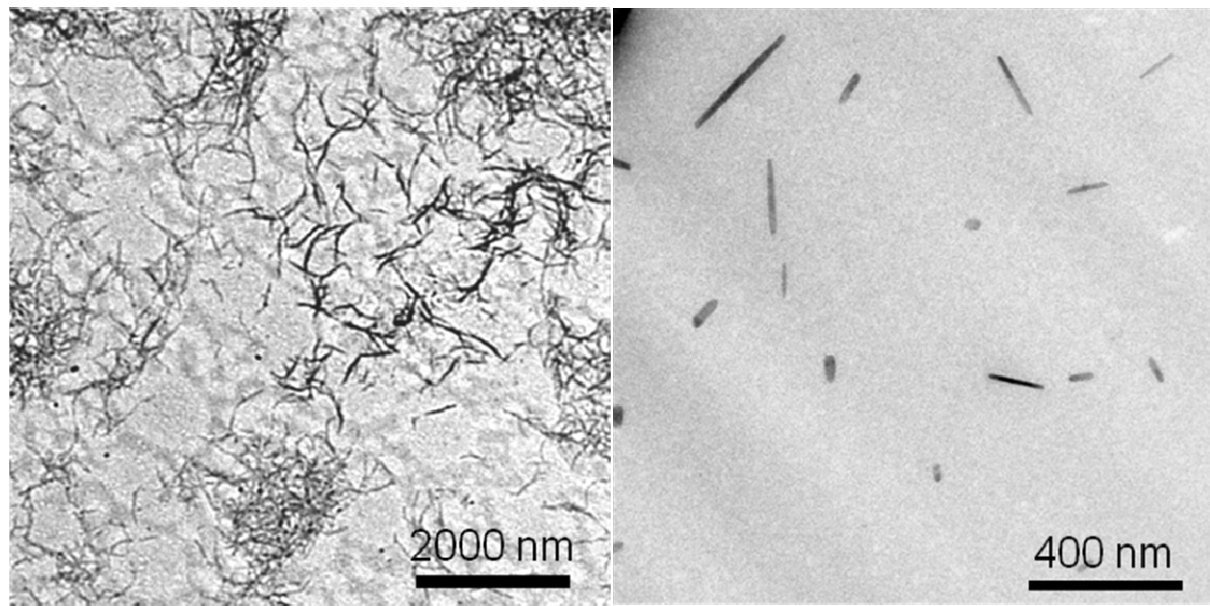


Fig. S2 Cryo-microtomy TEM images of the $[\text{Fe}(\text{NH}_2\text{-trz})_3](\text{tos})_2$ nano-structures observed after warming to 353 K in the magnetometer.

3.2. DLS measurements

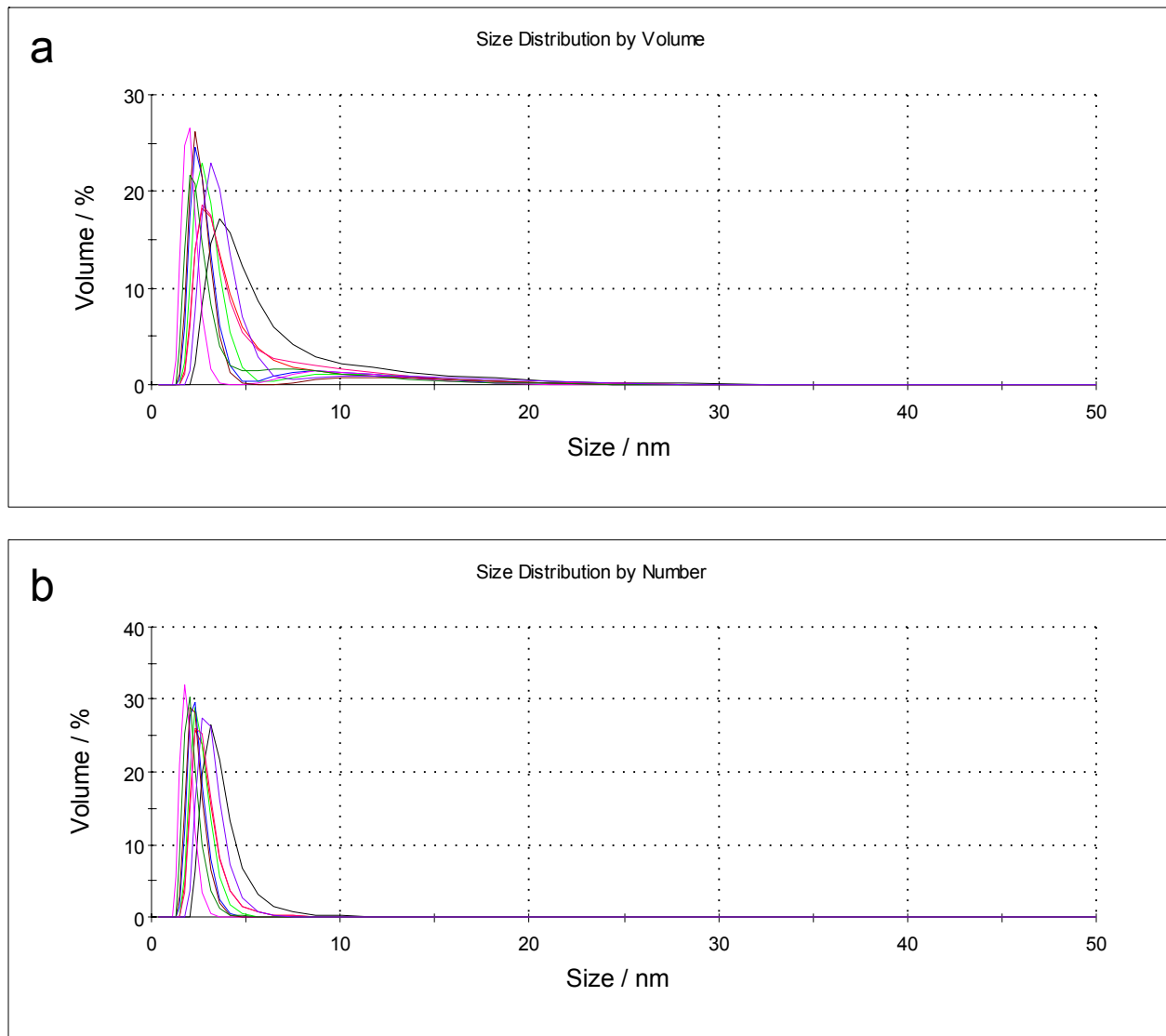


Fig. S3 Volume- (a) and number-based (b) particle size distribution for the colloidal suspension **I** at 293 K obtained by DLS analysis. (Parameters used for the data analysis: viscosity = 60 cP, refractive index = 1.450).

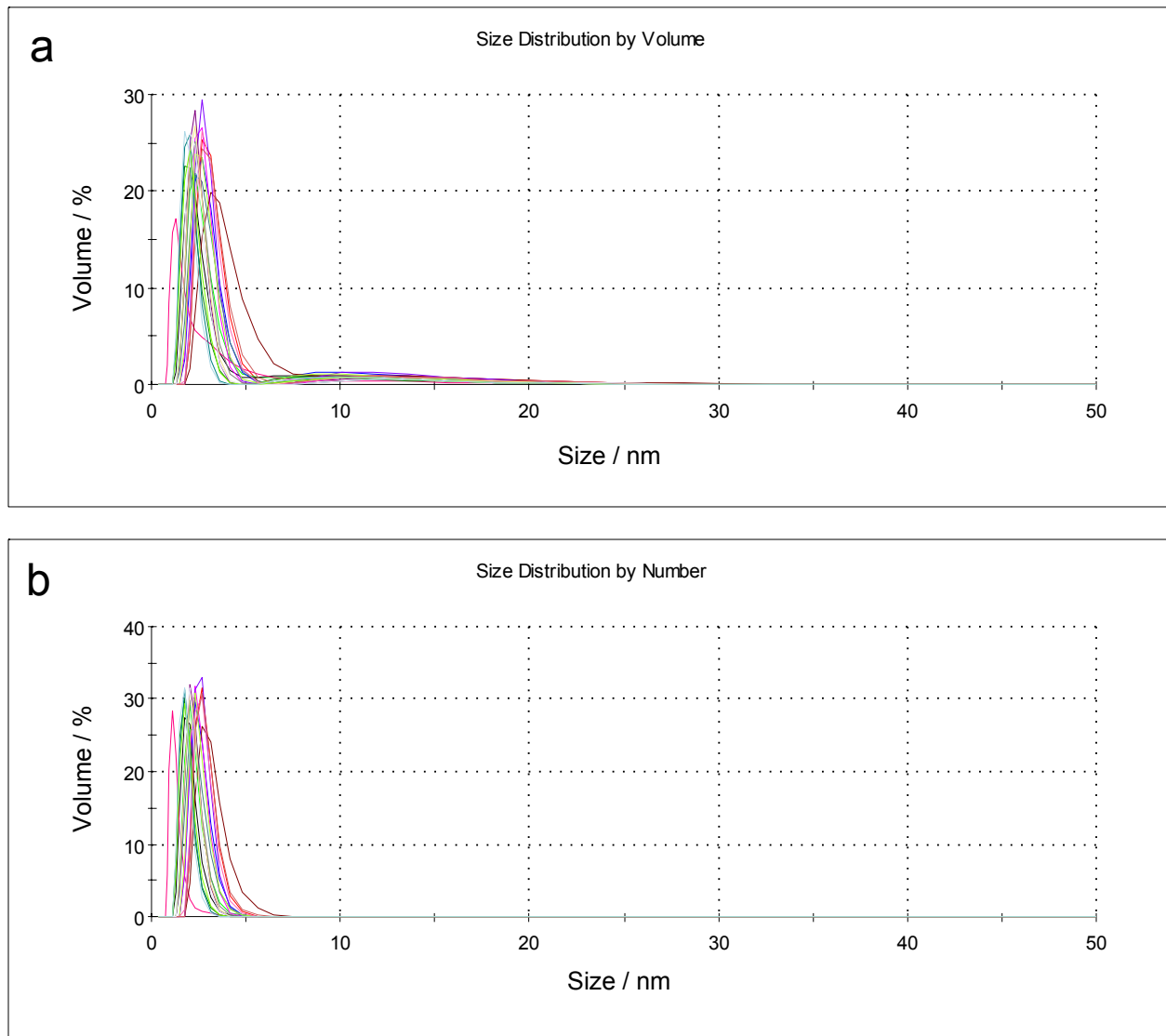


Fig. S4 Volume- (a) and number-based (b) particle size distribution for the colloidal suspension **I** isothermally held and measured by DLS analysis at 313 K. (Parameters used for the data analysis: viscosity = 21 cP, refractive index = 1.450).

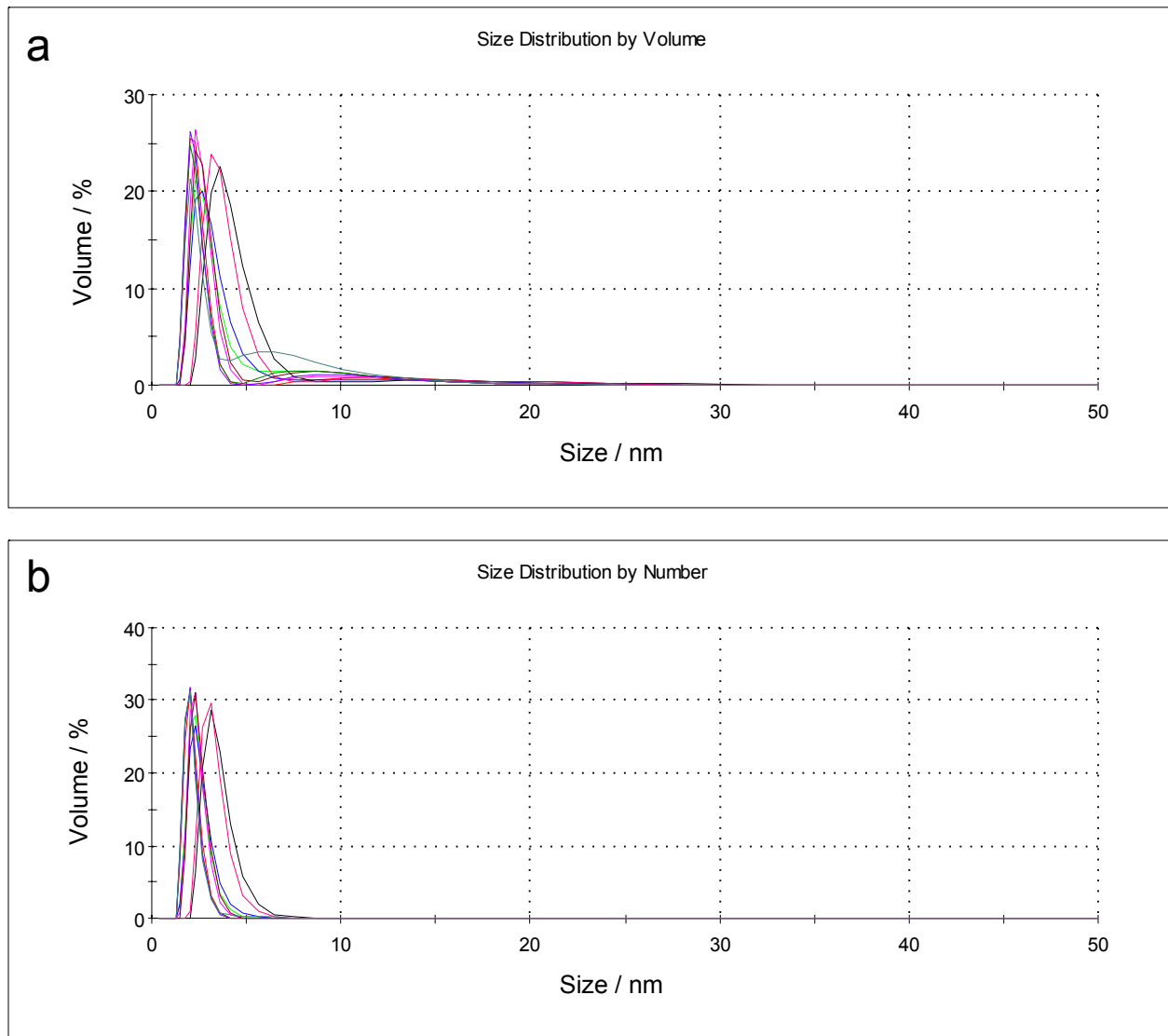


Fig. S5 Volume- (a) and number-based (b) particle size distribution for the colloidal suspension **I** measured by DLS analysis at 293 K after holding at 313 K. (Parameters used for the data analysis: viscosity = 60 cP, refractive index = 1.450).

3.3. UV absorption spectra

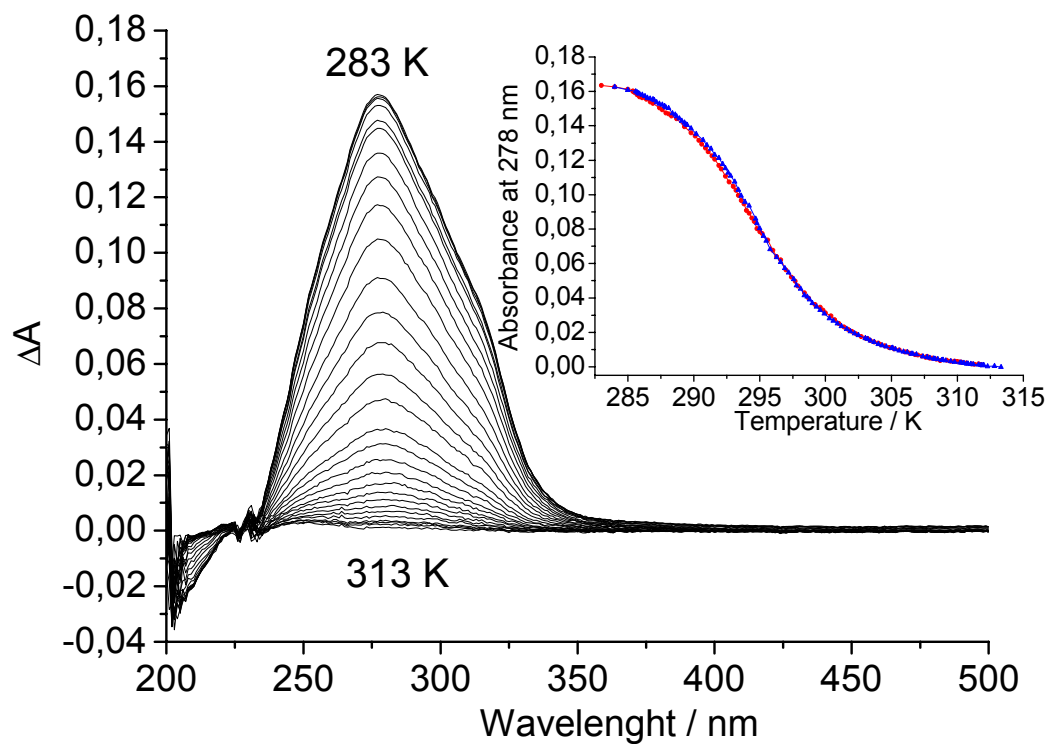


Fig. S6 Variable temperature absorption spectra obtained for *I* in the UV range, where $\Delta A = A_T - A_{T=313K}$. The inset displays the thermal dependence of the absorbance at 278 nm in the cooling (red) and heating (blue) modes.

3.4. Magnetic properties

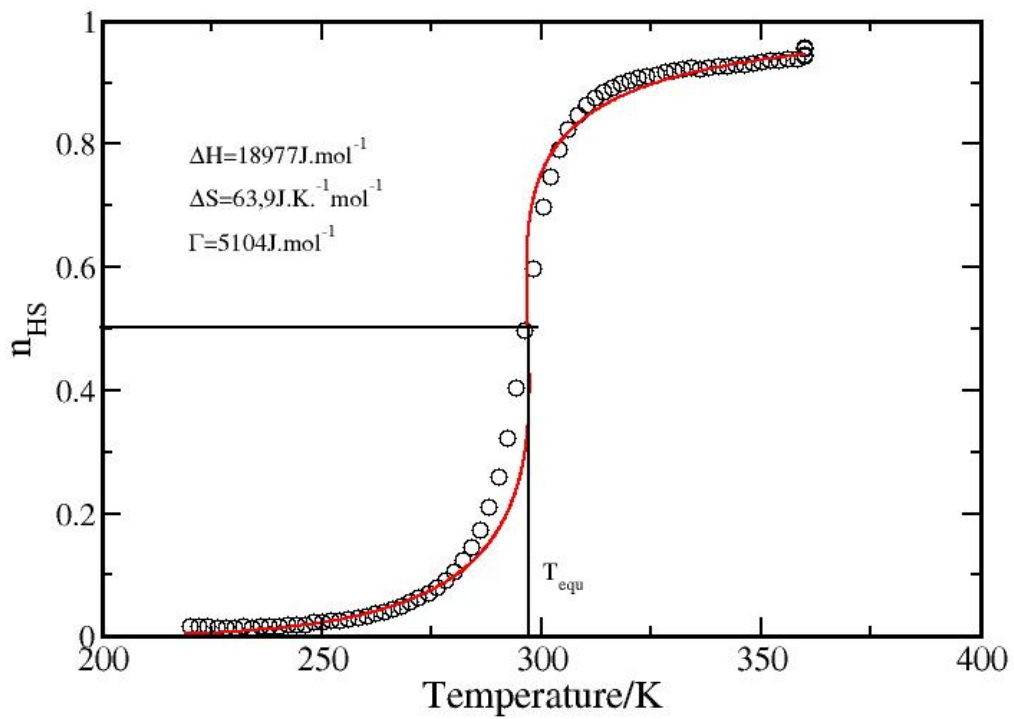


Fig. S7 Temperature dependence of the HS fraction for **I** in the heating mode from magnetic measurements: the open circles correspond to experimental data and the straight line represents the best fit obtained from the Slichter-Drickamer model. The inset gives the fitted thermodynamical parameters.

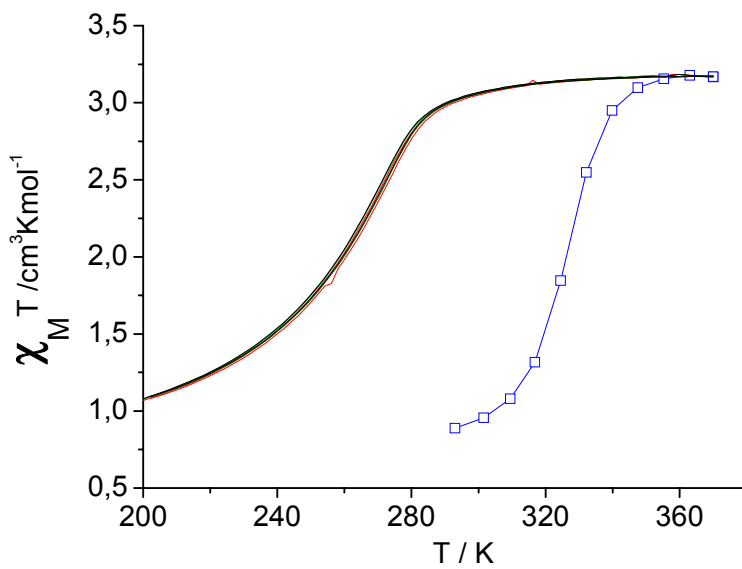


Fig. S8 Temperature dependence of $\chi_M T$ for **2** in the cooling and heating modes: the first heating (\square) is followed by 3 thermal cycles.

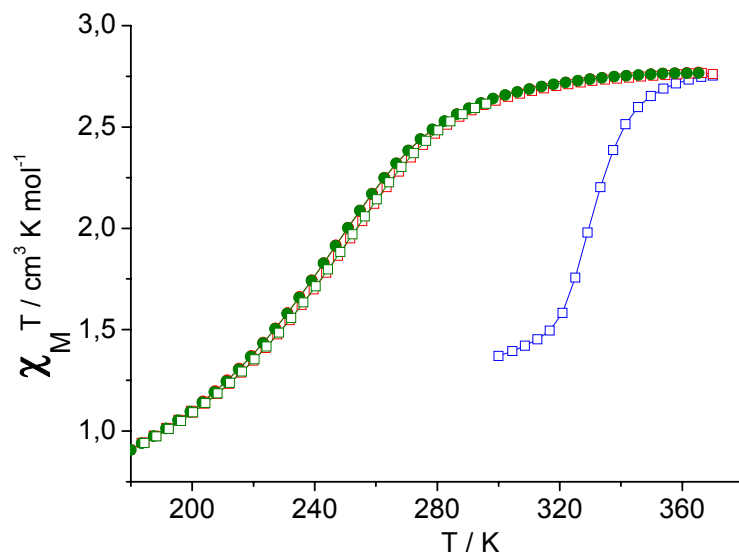


Fig. S9 Temperature dependence of $\chi_M T$ for $[\text{Fe}(\text{NH}_2\text{-trz})_3](\text{tos})_2$ bulk microcrystalline compound in the cooling and heating modes: first heating to 370 K (blue), first cycle between $180 \leftrightarrow 370$ K (red), second cycle between $180 \leftrightarrow 370$ K (green). The open squares correspond to heating and closed circles to cooling.

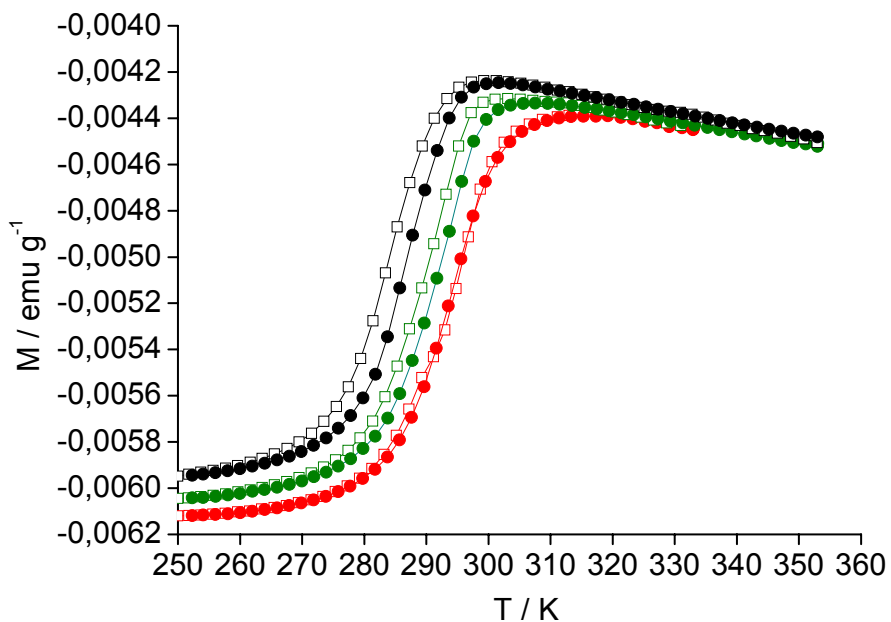


Fig. S10 Temperature dependence of the magnetization for *I* in the cooling and heating modes: first cycle between $250 \leftrightarrow 313$ K (red) - corresponding clearly to a colloidal dispersion with 3-4 nm particle size, second cycle between $250 \leftrightarrow 333$ K (green) and third cycle between $250 \leftrightarrow 353$ K (black). The open squares correspond to heating and closed circles to cooling.

3.5. Mössbauer spectra

Table 1. Hyperfine Mössbauer parameters (and their statistical errors) of iron(II) ions in sample 2 at 317 and 80 K (δ , ΔE_Q and Γ stand for the isomer shift (relative to metallic iron at room temperature), the quadrupole splitting and the half-height line width respectively).

T, K	HS doublet				LS doublet			
	δ , mm/s	ΔE_Q , mm/s	Γ , mm/s	Area, %	δ , mm/s	ΔE_Q , mm/s	Γ , mm/s	Area, %
317	0.9940 (20)	2.7221 (40)	0.1851 (33)	100	-	-	-	-
80	1.127 (11)	3.398 (22)	0.216 (19)	12.83 (96)	0.5056 (12)	0.2696 (20)	0.1636 (19)	87.17 (53)

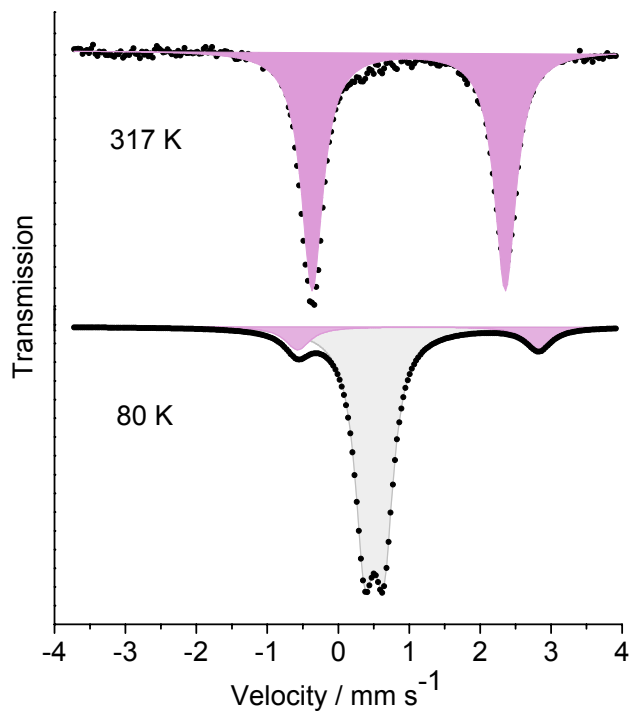


Fig. S11 ^{57}Fe Mössbauer spectra of sample 2 at 317 and 80 K. The solid lines represent fitted curves.

4. References

- 1 *Inorganic Syntheses*, ed. D. Coucouvanis, John Wiley & Sons, New York, 2002, vol. 33.
- 2 <http://www.malvern.com>.